

COMPARISON OF DEFECT CLUSTER ACCUMULATION AND PATTERN FORMATION IN IRRADIATED COPPER AND NICKEL – S.J. Zinkle and L.L. Snead (Oak Ridge National Laboratory), B.N. Singh (Risø National Laboratory), and D.J. Edwards (Pacific Northwest Laboratory)

OBJECTIVE

The objective of this study is to compare the contrasting behavior of defect cluster formation in neutron-irradiated copper and nickel specimens.

SUMMARY

Transmission electron microscopy was used to examine the density and spatial distribution of defect clusters produced in copper and nickel as the result of fission neutron irradiation to damage levels of 0.01 to 0.25 displacements per atom (dpa) at irradiation temperatures between 50 and 230°C (0.24 to 0.37 T_M in Cu). A high density of small stacking fault tetrahedra (SFT) and dislocation loops was observed in both materials, and a moderate density of small voids was observed in the copper specimens irradiated at 230°C. The visible defect cluster density in both materials approached a saturation value at doses >0.1 dpa. The visible defect cluster density in nickel was a factor of 5 to 10 lower than that in copper at all damage levels. The defect clusters in Ni organized into {001} walls at damage levels >0.1 dpa, whereas defect cluster alignment was not observed in copper. A comparison with published results in the literature indicates that defect cluster wall formation occurs in nickel irradiated at 0.2 to 0.4 T_M in a wide variety of irradiation spectra. Defect cluster wall formation apparently only occurs in copper during low temperature irradiation with electrons and light ions. These results are discussed in terms of the thermal spike model for energetic displacement cascades.

PROGRESS AND STATUS

1. Introduction

The effect of energetic displacement cascades on the microstructural evolution in metals is an interesting phenomenon for both fundamental and technological reasons. As reviewed elsewhere [1,2], the fraction of surviving defects (relative to the Kinchin-Pease calculated displacements) decreases with increasing primary knock-on atom (PKA) energy due to in-cascade recombination. On the other hand, in-cascade clustering produces a higher fraction of clustered defects under energetic displacement cascade conditions compared to low PKA energy irradiations. Due to the small size (~ 10 nm) and short lifetime ($\sim 10^{-11}$ s) of displacement cascades in metals, direct experimental investigation of individual cascades cannot be performed. Molecular dynamics (MD) simulations have been increasingly employed in recent years to provide some information on the evolution of the displacement cascade, including the distribution of clustered and isolated point defects [2-5]. Most of these MD studies have focused on copper due to the availability of realistic atomic potentials.

Copper and nickel are commonly used as model face-centered cubic metals in radiation effects studies. One useful approach for investigating radiation effects is to examine the fine-scale defect cluster formation in irradiated metals with transmission electron microscopy. Unfortunately, there is a lack of published information on the microstructure of copper and nickel irradiated to "moderate" doses (>0.01 dpa) at 50 to 300°C [44]. This temperature range corresponds to the transitional regime between recovery Stages III and V, which according to the one-interstitial model is associated with the initiation of vacancy migration and the thermal breakup of vacancy clusters, respectively.

Several experimental studies have noted that the small defect clusters produced in irradiated face-centered-cubic (FCC) metals such as Ni [6-15] and Cu [13,14] have a tendency to become aligned along {001} planes under certain conditions. The defect cluster alignment in Ni becomes noticeable at damage levels of ~ 0.1 displacements per atom (dpa), and remains stable up to damage levels in excess of 20 dpa. This alignment has been modeled on the basis of nonlinear diffusion-controlled coupling of point defects with

the defect structure [16,17]. These models have shown that defect cluster patterning ("self-organization") is expected when vacancy clusters are the dominant point defect sink [16,17]. In addition, the presence of specific orientation relationships between the defect cluster pattern and the host lattice was concluded to be due to anisotropic elastic strain fields around the defect clusters [16]. However, there has not yet been an attempt to systematically examine the effect of irradiation spectrum or material on defect cluster pattern formation.

The present study focuses on a comparison of the dose-dependent defect cluster density in neutron irradiated Cu and Ni (and their propensity to form aligned defect cluster patterns). Due to their similar mass and FCC crystal structure, Ni and Cu are attractive for studying fundamental aspects of irradiation, such as defect clustering processes associated with displacement cascades. Low energy ion irradiations [18-24] have demonstrated that a significantly higher density of visible vacancy clusters are produced in Cu compared to Ni over a wide range of irradiation temperatures. On the other hand, the amount of ion beam mixing [25] and the total surviving defect fraction (clustered and isolated point defects) associated with ion and neutron irradiation [26-29] have been found to be lower in Cu compared to Ni following irradiation near 4 K. These seemingly contradictory results have been interpreted as evidence for the presence of thermal spikes in displacement cascades. According to the thermal spike model, the lower melting point and weaker electron-phonon coupling in Cu compared to Ni both act to increase the duration and affected volume of the liquid-like region associated with a displacement cascade [3, 21-25]. The relatively large volume and slow cooling rate for the thermal spike in Cu promotes point defect recombination and leads to more pronounced clustering of the surviving defects. One criticism of the low energy ion irradiation studies is that the cascades are produced close to the specimen surface, and therefore the surface may be exerting some influence over the visible cluster formation. In addition, it is possible that the implanted ions in these low-energy irradiations may influence the details of the cluster formation process. One of the objectives of the present study was to examine the defect cluster formation process in neutron-irradiated specimens to determine if the trends observed in the ion irradiation studies are also observed under bulk irradiation conditions.

Further support for the thermal spike model was obtained in some limited MD studies that compared the response of Cu and Ni to low energy (<5 keV) PKA irradiations [3-5]. The calculated fraction of defects that survived the cascade quench was lower in copper, and the relative proportion of defects contained in clusters for a given PKA energy was higher in copper compared to nickel, in agreement with the ion beam mixing, surviving defect fraction, and vacancy loop production experimental measurements. Similar results were also obtained with a heat equation model that used an initial displacement cascade energy distribution obtained from binary collision calculations [30,31].

2. Experimental Procedure

The materials used in this investigation were 99.99% (VP grade) nickel obtained from Materials Research Corporation and oxygen free high-conductivity copper. The major impurities in the nickel were 37 ppm C, 18 ppm O, 25 ppm Fe, 25 ppm Si, 10 ppm Cu and 10 ppm Mn. Transmission electron microscope (TEM) disks with a diameter of 3 mm were punched from nickel and copper sheets of thickness 200 μm and 100 μm , respectively. The TEM disks were recrystallized by vacuum annealing at 750°C and 550°C for 2 h for the nickel and copper disks, respectively.

Two different fission reactors were used for the irradiations. The High Flux Isotope Reactor (HFIR) irradiations were performed in the HT-3 hydraulic rabbit tube facility with a fast neutron flux of 7.8×10^{18} $\text{n/m}^2\text{-s}$ ($E > 0.1$ MeV) and a thermal neutron flux of 2.2×10^{18} $\text{n/m}^2\text{-s}$, which produced a calculated [32] damage rate of 7.2×10^{-7} dpa/s in copper, assuming a threshold displacement energy of 30 eV. Specimens were irradiated at a temperature of 230°C in separate capsules for time periods of 4.6, 46 and 115 hours. Further details of the HFIR irradiations are given elsewhere [15]. The DR-3 irradiations were performed at a temperature of 50°C at approximately an order of magnitude lower damage rate (5×10^{-8} dpa/s) compared to the HFIR irradiations. The HFIR and DR-3 irradiation conditions are summarized in Table 1. The displacement damage levels ranged from 0.01 to 0.25 dpa.



Fig. 1. Comparison of the general microstructure of copper following neutron irradiation at 230°C to a damage level of 0.012 dpa (top) and 0.12 dpa (bottom). The beam direction is near $\langle 110 \rangle$ in both micrographs.

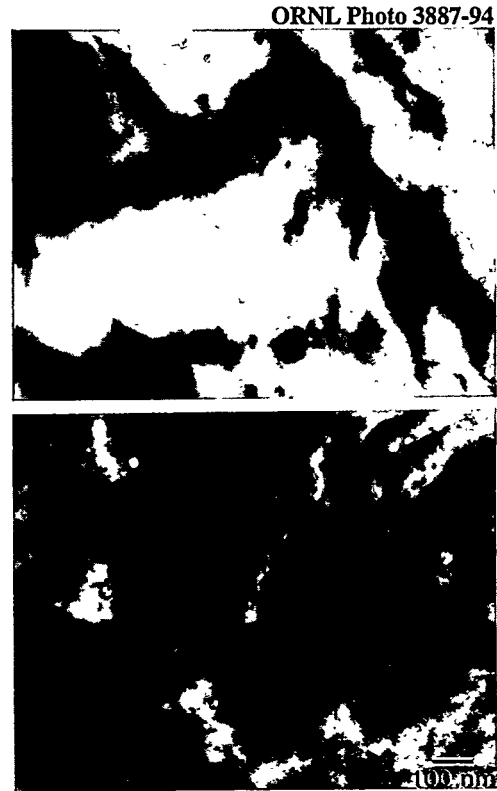


Fig. 2. Cavity formation observed in copper following neutron irradiation at 230°C to a damage level of 0.012 dpa (top) and 0.12 dpa (bottom).

Table 1. Summary of Neutron Irradiation Conditions

Material	Reactor	Temperature (°C)	Damage Levels (dpa)
Cu	HFIR	230	0.01, 0.1
Cu	DR-3	50	0.01, 0.1, 0.2
Ni	HFIR	230	0.1, 0.25

The TEM disks were jet-electropolished following irradiation, and examined in JEOL 2000FX electron microscopes located at Risø and Oak Ridge National Laboratories. A combination of conventional bright field and weak beam dark field (WBDF) techniques were used to examine the defect microstructure. The general microstructural features, including void formation, network dislocation density and the presence or absence of defect cluster patterning, was performed in regions with a typical thickness of 100 to 150 nm. The density and size of the small "black spot" defect clusters was obtained from WBDF (g,4g or g,5g diffraction conditions) micrographs taken in regions with a typical foil thickness of <40 nm. The foil thickness was determined from the number of weak beam fringes.

3. Results

The unirradiated microstructure of both the copper and nickel specimens was typical of annealed single-phase metals, with a grain size of $\sim 100 \mu\text{m}$ and a dislocation density of $\sim 10^{12}/\text{m}^2$. Irradiation introduced fine defect structures. Figure 1 shows the general microstructure of the two copper specimens irradiated in HFIR to damage levels of 0.01 and 0.1 dpa. A heterogeneous network dislocation density of $\sim 6 \times 10^{12}/\text{m}^2$ was present in both specimens. There was no evidence of aligned defect clusters or defect cluster wall formation in either of the irradiated copper specimens. A low density ($< 1 \times 10^{20}/\text{m}^3$) of dislocation loops

with diameters >5 nm is also visible at both doses in Fig. 1. A similar low network dislocation density was also observed in the copper specimens irradiated in DR-3 at 50°C.

The major radiation-induced microstructural feature of the copper specimens irradiated in DR-3 at 50°C was a high density of small defect clusters. The network dislocation density was $\sim 10^{12}/\text{m}^2$ at all three doses of 0.01, 0.1, and 0.2 dpa. The measured density of small defect clusters was $5.3 \times 10^{23}/\text{m}^3$ after 0.01 dpa, $6.7 \times 10^{23}/\text{m}^3$ after 0.1 dpa, and $6.6 \times 10^{23}/\text{m}^3$ after 0.2 dpa. Greater than 60% of the defect clusters were resolvable as SFTs at both doses. The mean defect cluster size was ~ 2.5 nm. There was no evidence for defect cluster alignment at any dose in the DR-3 specimens.

A moderate density of small voids was observed in both of the copper specimens irradiated in HFIR at 230°C. Figure 2 compares the void microstructures in copper irradiated at 230°C to 0.01 and 0.1 dpa. The void distribution appeared to coarsen with increasing dose. The measured void density decreased from $3 \times 10^{20}/\text{m}^3$ at 0.01 dpa to $1 \times 10^{20}/\text{m}^3$ at 0.1 dpa, and the corresponding average void diameter increased from 10 nm to 27 nm. The volumetric swelling calculated from the void measurements was $\sim 0.01\%$ at 0.01 dpa and $\sim 0.1\%$ at 0.1 dpa. The measured void densities at 0.01 and 0.1 dpa are similar to densities previously reported for copper irradiated with neutrons near 250°C at higher doses of 0.1 to 1 dpa [44], indicating that void nucleation in copper is completed at temperatures of 230 to 250°C after damage levels of ~ 0.01 dpa.

Figure 3 shows an example of the high density of small defect clusters observed in copper following HFIR irradiation at 230°C to 0.01 and 0.1 dpa. The measured defect cluster density was $\sim 1.6 \times 10^{23}/\text{m}^3$ at both irradiation doses, which suggests that the cluster density had reached a saturation level already at 0.01 dpa. The fraction of the total defect cluster density identified as stacking fault tetrahedra was between 90 and 95% for both irradiation doses. The mean defect cluster size (predominantly SFTs) was about 2.5 nm at both damage levels, in agreement with previous studies on neutron-irradiated copper [35,53-56].

A high density of small defect clusters was observed in nickel following irradiation. The measured defect cluster density was $1.9 \times 10^{23}/\text{m}^3$ after 0.1 dpa, and $2.0 \times 10^{23}/\text{m}^3$ after 0.25 dpa. Typical microstructures for the two damage levels are shown in Fig. 4. About 33% of the defect clusters were resolvable as SFTs in the 0.1 dpa specimen, and this fraction decreased to about 28% in the 0.25 dpa specimen. In addition, the fraction of defect clusters that were resolvable as dislocation loops on $\{111\}$ habit planes increased slightly from 50% to 60% as the dose increased from 0.1 to 0.25 dpa. The remaining 12 to 17% of the defect clusters at the two damage levels could not be unambiguously identified due to their small size. The average size of the visible SFTs was about 2 nm at both doses, whereas the average diameter of the resolvable $\{111\}$ loops increased from 5.4 nm to 6.6 nm as the dose increased from 0.1 to 0.25 dpa. This caused the total defect cluster mean size to increase from 3.5 to 4.3 nm with increasing dose. Previous studies have reported similar average SFT sizes of ~ 2 nm in nickel irradiated with neutrons at a comparable temperature of 200°C [57]. Average interstitial loop sizes as large as ~ 60 nm have been reported for Ni irradiated with neutrons at 200°C to a dose of ~ 0.01 dpa at a low damage rate [58].

In contrast to the pure copper results, the dislocation density in nickel increased considerably after neutron irradiation. The measured network dislocation density in Ni varied from $\sim 1 \times 10^{14}/\text{m}^2$ for the 0.1 dpa specimen to $\sim 5 \times 10^{13}/\text{m}^2$ for the 0.25 dpa specimen. Figure 5 shows the general microstructure of nickel following irradiation to a damage level of 0.1 dpa. There was some alignment of the small defect clusters into a $\{100\}$ planar wall configuration in the 0.1 dpa specimen. The defect cluster alignment became more pronounced after irradiation to a damage level of 0.25 dpa, as indicated in Fig. 6. The average spacing between the $\{100\}$ walls of defect clusters was about 45 nm. The network dislocations did not show any tendency toward alignment at either irradiation dose. Cavity formation was not observed in either of the irradiated nickel specimens.

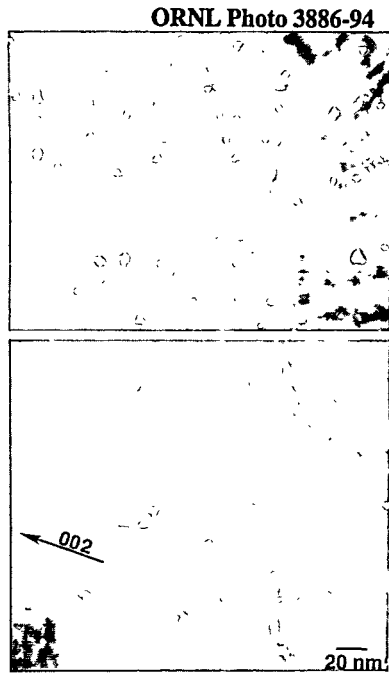


Fig. 3. Weak beam (g,4g) $g=002$ micrograph of small defect clusters produced in copper during irradiation at 230°C to a damage level of 0.012 dpa (top) and 0.12 dpa (bottom). The beam direction is near $\langle 110 \rangle$ in both micro-graphs, and the direction of the diffraction vector is indicated on the bottom micrograph.

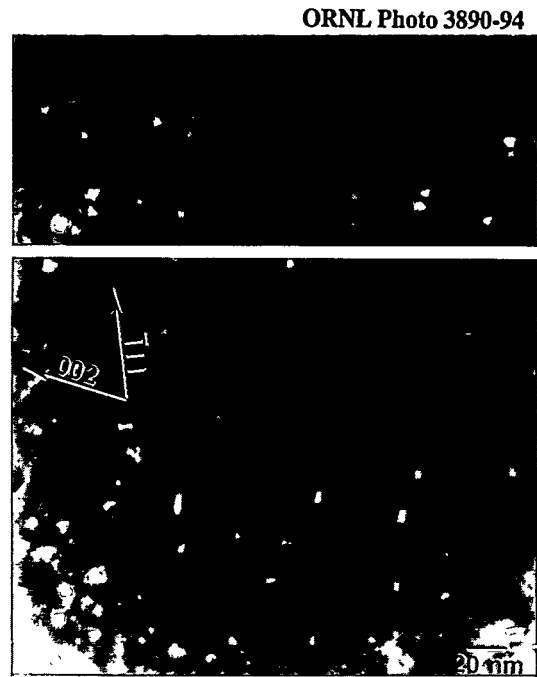


Fig. 4. Weak beam (g,4g) $g=002$ micrograph of small defect clusters produced in nickel during irradiation at 230°C to a damage level of 0.1 dpa (top) and 0.25 dpa (bottom). The beam direction is near $\langle 110 \rangle$ in both micrographs.

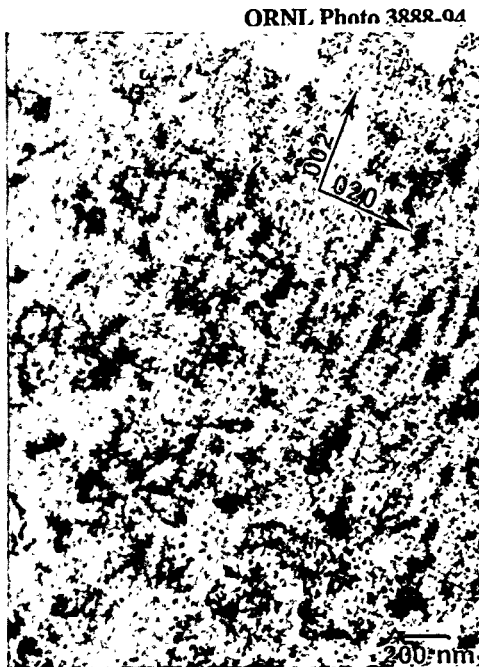


Fig. 5. Dislocations and defect clusters in nickel following neutron irradiation at 230°C to a damage level of 0.1 dpa. The beam direction is near $\langle 100 \rangle$.



Fig. 6. Network dislocations and aligned defect clusters in nickel following irradiation to a damage level of 0.25 dpa. The beam direction is near $\langle 110 \rangle$.

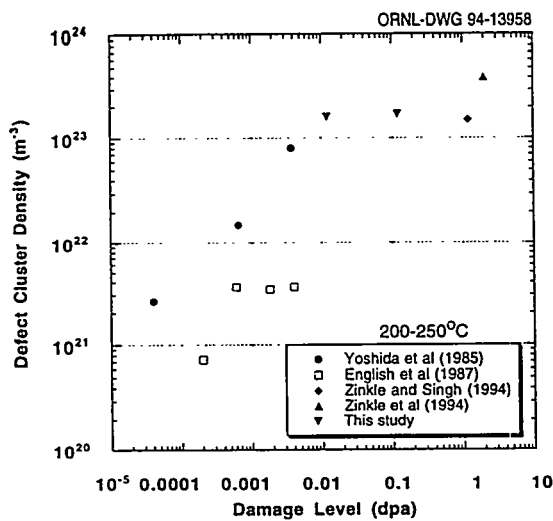


Fig. 7. Dose-dependent defect cluster formation in copper following irradiation at 200 to 250°C [33,59-61].

4. Discussion

Figure 7 compares the defect cluster densities measured in copper in this study with previously reported data [33,59-61] in the same irradiation temperature range of 200 to 250°C. These results suggest that the defect cluster density approaches a saturation value of $\sim 2 \times 10^{23}/\text{m}^3$ after an irradiation dose of only 0.01 dpa at $\sim 230^\circ\text{C}$. High dose studies performed on copper at other temperatures have found that the defect cluster density approaches a saturation value near $1 \times 10^{24}/\text{m}^3$ after irradiation to damage levels >0.1 dpa near room temperature, and this saturation defect cluster density decreases rapidly with increasing neutron irradiation temperature above $\sim 150^\circ\text{C}$ [33,44]. The decrease in the saturation defect cluster density in Cu at neutron irradiation temperatures above $\sim 150^\circ\text{C}$ ($0.31 T_M$) may be attributed to thermal evaporation of SFTs. The detailed quantitative behavior of the SFT density at elevated temperatures depends on the balance between their production in displacement cascades and their subsequent shrinkage. At very high damage rates typically encountered in ion irradiation experiments ($\sim 10^{-3}$ dpa/s), the vacancy cluster lifetime is controlled by interstitial annihilation events [62]. At damage rates typical for neutron irradiations ($<10^{-6}$ dpa/s), the vacancy cluster lifetime is controlled by thermal evaporation. In both cases, however, the quantitative value of the defect cluster density at elevated temperatures depends on the damage rate [62].

One striking feature associated with copper is that the defect cluster size and geometry at temperatures up to $\sim 200^\circ\text{C}$ is remarkably insensitive to irradiation dose. Previous irradiation studies performed at damage rates near 10^{-8} to 10^{-7} dpa/s have found that the SFT fraction is 60 to 65% of the total defect cluster density in copper irradiated at $\sim 200^\circ\text{C}$ to damage levels between 5×10^{-5} dpa and 2 dpa [33,59-61]. The SFT fraction approaches 100% of the defect cluster density at higher irradiation temperatures [61,63]. In the present study, the measured SFT fraction was approximately 90% of the total defect cluster density following irradiation at 230°C at both 0.01 and 0.1 dpa. The average size of SFTs in Cu has been found to be 2 to 3 nm over a very wide range of damage levels (10^{-5} to 10 dpa) and temperatures (20 to 300°C) density in nickel irradiated at "low" temperatures ($<0.3 T_M$) is five to ten times lower than that in copper at all damage levels from 10^{-4} dpa to ~ 1 dpa (see Fig. 12). For example, the defect cluster density in Cu reaches an apparent saturation value of $\sim 1.0 \times 10^{24}/\text{m}^3$ for damage levels >0.1 dpa at homologous neutron irradiation temperatures $<0.31 T_M$ [44], whereas the measured defect cluster density in Ni irradiated at $0.29 T_M$ to damage levels of 0.1 and 0.25 dpa in the present study was only $\sim 2.0 \times 10^{23}/\text{m}^3$ (Fig. 8).

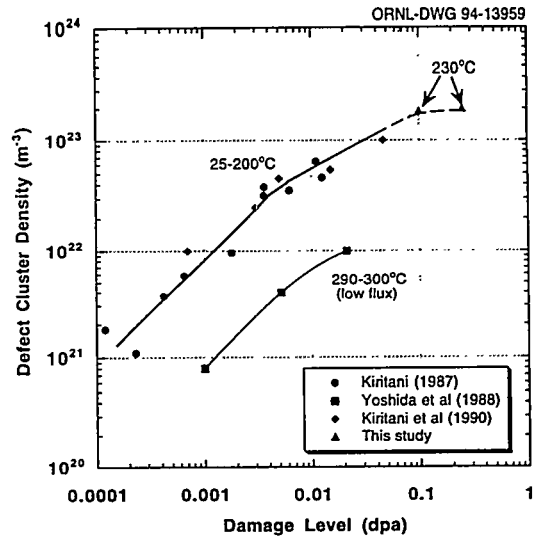


Fig. 8. Dose-dependent defect cluster formation in nickel following neutron irradiation at 25 to 300°C [64-66].

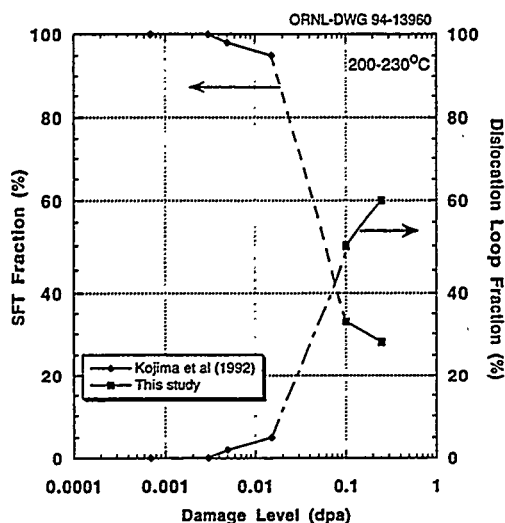


Fig. 9. Evolution of the defect cluster morphology in irradiated nickel at 200 to 230°C [58].

Figure 8 summarizes the dose dependence of the defect cluster density in nickel following irradiation at temperatures between room temperature and 300°C [64-66]. The data indicate that the defect cluster density accumulation is independent of irradiation temperature up to at least 200°C (0.27 T_M). Furthermore, the data suggest that the defect cluster density in nickel reaches an apparent saturation value of $\sim 2 \times 10^{23}/m^3$ after irradiation to doses above 0.1 dpa at low temperatures ($< 0.30 T_M$). A significantly lower defect cluster accumulation rate occurred during low flux ($\sim 10^{-8}$ dpa/s) irradiation at temperatures near 300°C (0.33 T_M). The defect cluster densities measured in the two specimens irradiated to 0.1 and 0.25 dpa at 230°C in the present study are the highest defect cluster densities reported to date for neutron irradiated nickel. Since the irradiation temperature of 230°C (0.29 T_M) is close to the temperature where SFTs would be expected to be thermally unstable in nickel, it is uncertain if a defect cluster density somewhat higher than $2 \times 10^{23}/m^3$ would be produced by high dose irradiation at lower temperatures. It is interesting to note that the visible defect cluster appears to be most pronounced at damage levels between 0.01 and 0.1 dpa. Further study is needed to confirm this apparent pronounced evolution from an SFT-dominant microstructure to a dislocation loop-dominant microstructure.

When the present results are considered along with previously reported data on irradiated copper and nickel, several material-dependent differences are evident. First, the total defect cluster density observed in copper at homologous temperatures below 0.3 T_M is a factor of five to ten higher than that observed in irradiated nickel (Fig. 12). Second, the density of dislocation loops and network dislocations in copper is very low at all irradiation conditions [33,35,61,63]. The loop and network dislocation density in copper is at least an order of magnitude lower than that observed in nickel at comparable irradiation conditions for doses > 0.1 dpa. The low density of loops and network dislocations in copper appears to be related to difficulties in interstitial loop nucleation. This is reflected in the insensitivity of the copper SFT and loop fractions to the displacement damage level. It is possible that the high sink density in copper associated with the SFTs produced in displacement cascades may inhibit interstitial loop nucleation and growth at temperatures up to $\sim 0.3 T_M$. However, studies performed on copper irradiated at higher temperatures have shown that the interstitial loop density is also very low at 0.3 to 0.5 T_M (where the sink density associated with SFTs is low) [35,61,63].

It is interesting to note that a well-developed network dislocation density is not needed to achieve high void swelling rates ($> 0.5\%/dpa$) in copper. According to standard rate theory models, the highest void swelling rates in metals such as copper and nickel would be expected to occur in the presence of moderate dislocation densities of $\sim 10^{14}/m^2$ [67]. These moderate dislocation densities produce a point defect sink density that is comparable to the sink density at voids, and the preferential absorption of interstitials at

In contrast to the behavior of copper, the morphology of the defect clusters in nickel exhibits an apparent strong dependence on irradiation dose. Figure 9 shows the effect of irradiation dose on the dislocation loop and SFT fractions in nickel irradiated at 200 to 230°C [58]. Although only a limited amount of data are available, the results indicate that there is a gradual change from a SFT-dominant microstructure at low doses to an interstitial dislocation loop-dominant microstructure at high doses. The microstructural evolution following heavy ion, 600 to 750 MeV proton, or fission or fusion neutron irradiation [33,34,35,53-56,59-61]. The insensitivity of SFT size in Cu to irradiation temperature and dose may be attributed to their direct formation in energetic displacement cascades, as opposed to a classical monovacancy nucleation and growth process.

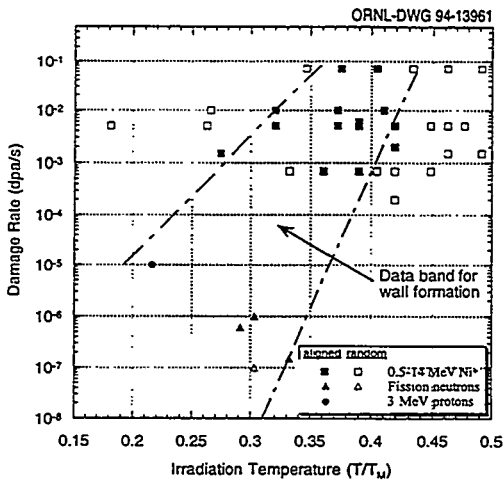


Fig. 10. Data compilation showing the temperature and dose rates where {001} defect cluster wall formation has been observed in irradiated nickel. The data include Ni⁺ ion [6,7,10-12], fission neutron [8,9,15, this study], and proton [13,14] irradiations. The filled symbols denote conditions where defect cluster wall formation was observed.

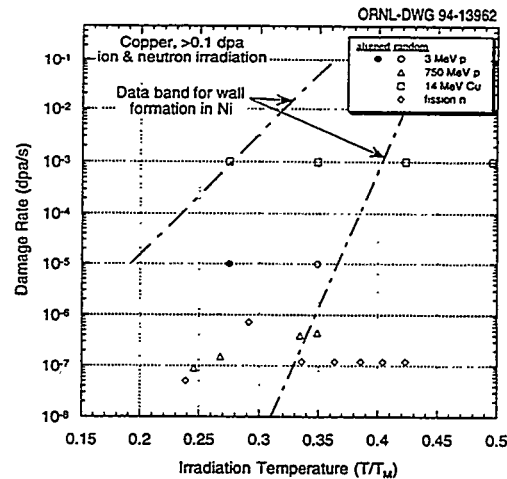


Fig. 11. Microstructural observations of the absence (open symbols) or presence (filled symbol) of aligned defect cluster walls in irradiated copper. The dashed lines outline the data band for observations of wall formation in irradiated nickel (Fig. 5). The Cu data include 3-MeV protons [13,14], 750-MeV protons [33], Cu⁺ ions [34] and fission neutrons [15, 35, this study].

dislocations (dislocation bias) provides a vacancy supersaturation that is sufficient to sustain high levels of void swelling. Significant amounts of void swelling ($\sim 0.5\%/dpa$) have been observed in copper irradiated at 220 to 400°C despite network dislocation densities $< 10^{13}/m^2$ [35,61,68,69]. On the other hand, nickel apparently exhibits a very low steady-state swelling rate ($\sim 0.1\%/dpa$) in the presence of a network dislocation density of $\sim 2 \times 10^{13}/m^2$ after an initial high-swelling transient [70]. The high amount of swelling in the presence of a low dislocation density in neutron-irradiated copper can be reconciled by invoking the recently developed "production bias" model [71,72]. This model recognizes that a sufficiently high vacancy supersaturation to support significant void swelling can be achieved even in metals with low dislocation densities, due to the preferential loss of small interstitial clusters that are formed in displacement cascades by one-dimensional glide to dislocations and permanent sinks such as grain boundaries.

4.1 Defect cluster wall formation

The formation of periodic walls of defect clusters in irradiated metals has been reviewed elsewhere [16], and is part of a more general self organization process that occurs under certain irradiation conditions [17]. In the present study, defect cluster alignment into {001} planar walls began to occur in the neutron irradiated Ni specimens at an irradiation dose of 0.1 dpa, and was easily visible (but not completely developed) by 0.25 dpa. The observed 45 nm spacing between the {001} walls in the present study agrees well with previous results obtained in nickel following neutron and ion irradiation [16].

In order to make a better assessment of the similarities and differences between irradiated nickel and copper regarding their propensity to form aligned defect cluster walls during irradiation, we have compiled the pertinent studies into plots showing the temperature and dose rates where {001} defect cluster walls have been observed in irradiated nickel and copper. As shown in Fig. 10, defect cluster patterning occurs in nickel at homologous irradiation temperatures between 0.2 and 0.42 T_M (depending on the dose rate) [6-15]. These studies have found that wall formation in Ni becomes observable at damage levels > 0.1 dpa, and is fully developed by 0.5 to 1 dpa [15,16]. One important feature is that the defect clusters contained in the {001} walls are vacancy in nature [16]. From a theoretical viewpoint, self-organization of defect clusters into aligned patterns is expected only when the vacancy clusters are the dominant sink for interstitials and vacancies [16,17]. Defect cluster alignment is generally not observed at high irradiation temperatures due to thermal dissolution of vacancy clusters (recovery Stage V) [16]. The physical

mechanism responsible for the apparent lack of defect cluster patterning at low temperatures (Fig. 10) is not as clear. It has been proposed [16] that defect cluster ordering is suppressed at low temperatures and high damage rates because point defect matrix recombination becomes the dominant annihilation mechanism (as opposed to annihilation at defect clusters). However, according to the microstructural observations in the present study, the sink strength associated with defect clusters in neutron or ion irradiated nickel should be $>10^{15}/\text{m}^2$ at these low temperatures (since the defect clusters are produced directly in the displacement cascade, the cluster density is only weakly dependent on irradiation temperature [20,22]). It is difficult to imagine that annihilation could occur predominantly via point defect matrix recombination in the presence of such a high sink strength.

Figure 11 shows the corresponding dose rate-temperature plot for defect cluster patterning in irradiated copper [13-15,33-35]. The most striking feature in this plot is the lack of defect cluster wall formation in copper at irradiation conditions which caused significant {001} wall formation in nickel. Neglecting electron irradiation studies which will be discussed later, defect cluster wall formation has only been observed in copper irradiated with 3-MeV protons [13,14]. In some cases such as the present study, the accumulated dose (0.1 dpa) may have been too low to allow the full development of defect cluster patterning. However, some evidence of pattern formation should have been detectable, since evidence for wall formation was observable in Ni already at damage levels of 0.1 dpa (Fig. 5).

Several different studies have observed the presence of aligned defect clusters in copper [36-40] and nickel [40] following electron irradiation. Regular arrays of SFTs along $\langle 001 \rangle$ have been observed in copper during electron irradiation at temperatures between 170 and 350 K (0.12 to 0.26 T_M) and in nickel at temperatures between 380 and 540 K (0.22 to 0.31 T_M) [40]. In summary, it appears that defect cluster patterning occurs readily in nickel in irradiation spectra ranging from high PKA energies (Ni⁺ ion and neutron) to low PKA energies (3 MeV protons and 1 MeV electrons). On the other hand, copper apparently only forms defect cluster patterns in irradiation spectra that produce low PKA energies.

One possible explanation for the contrasting behavior of copper and nickel regarding defect cluster patterning is associated with their contrasting displacement cascade (thermal spike) behavior. As mentioned in the introduction, experimental and MD studies have demonstrated that considerable differences exist in the defect production and in-cascade clustering for energetic cascades in Cu versus Ni. Table 2 summarizes experimental measurements on the surviving defect fraction and the fraction of visible vacancy clusters per cascade (defect cluster yield) in copper and nickel irradiated with ions or neutrons [18-24,26-29]. The surviving defect fraction (fraction of the modified Kinchin-Pease displacements) was determined from in-situ electrical resistivity measurements during fission or 14-MeV neutron irradiation at temperatures near 4 K [26-29]. Since defect migration in Cu or Ni is not possible at this low temperature, these measurements include all defects (clustered or isolated point defects) that remain following the cascade quench. The data summarized in Table 2 have in some cases been modified from the originally published values in order to consistently use the recommended [41] threshold displacement energies of 30 eV for Cu and 40 eV for Ni and Frenkel pair electrical resistivities [27] of 2.0 and 6.0 $\mu\Omega\text{-m}$ for Cu and Ni, respectively. The surviving defect fraction measurements indicate that the total number of defects remaining after the cascade quench is equal or slightly higher in nickel compared to copper. The defect cluster yield measurements summarized in Table 2 were obtained from in-situ TEM analysis of thin specimens that were irradiated at 30 K or room temperature with either 50 keV Kr⁺ ions, 50 keV Ni⁺ ions or 30 keV Cu⁺ ions [18-20,22,24], and is a measure of the fraction of defects that survive the cascade quench in the form of vacancy clusters. The ion irradiation conditions selected for Table 2 produce displacement cascades that equal or exceed the threshold PKA energy for subcascade formation [42]. The absolute values for the defect yield measured by different workers have an uncertainty of about ± 0.1 due to differences in the counting procedure [23], but the general trend for higher in-cascade production of vacancy clusters in copper compared to nickel at all temperatures is unmistakable.

Due to the close proximity of the surface to the displacement cascades created by the 30 to 50 keV ion irradiations, the defect yield measurements summarized in Table 2 only contain information on vacancy clusters [21,23, 43]. Some information about interstitial clustering can be obtained from TEM studies on neutron-irradiated bulk specimens [43], although it must be recognized that many of the interstitial clusters

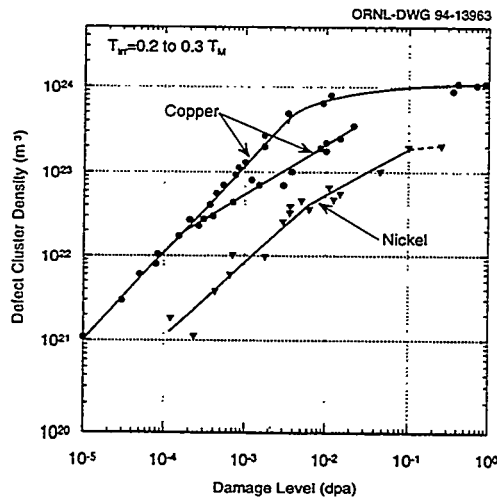


Fig. 12. Comparison of the dose-dependent defect cluster density in nickel and copper irradiated at low temperatures. Details about the original references are given elsewhere [15,44].

The saturation defect cluster density is apparently a factor of 5 lower in nickel compared to copper ($2 \times 10^{23}/\text{m}^3$ vs. $1 \times 10^{24}/\text{m}^3$). The fraction of defects resolvable of SFTs (vacancy clusters) in Cu and Ni ranges between 50 and 90%, depending on dose. Therefore, the neutron irradiation measurements are consistent with the ion irradiation defect yield studies (Table 2) that vacancy cluster production is higher in copper compared to nickel.

Table 2. Comparison of the total [26-29] and visible (clustered) [18-20,22,24] defect fractions. The surviving defect fraction was obtained from electrical resistivity measurements on neutron irradiated specimens, and the defect cluster yield was obtained from in-situ TEM measurements on specimens irradiated with 30 to 50 keV self- or Kr⁺-ions.

Total Surviving Defect Fraction at 4 K (NRT dpa fraction)		Visible Defect Cluster Yield (Observed # of Clusters per Cascade)	
		30 K	300 K
Cu	0.32	0.20	0.44
Ni	0.34	0.10	0.22

A further difference between the microstructure of neutron irradiated copper and nickel is apparent at damage levels of ~ 0.1 dpa. The interstitial dislocation loop size and density in nickel irradiated at homologous temperatures between 0.2 and 0.3 T_M increase steadily with increasing dose, and the loop density exceeds the SFT density ($1 \times 10^{23}/\text{m}^3$) at damage levels greater than about 0.1 dpa [15]. On the other hand, the resolvable (>5 nm diameter) interstitial loop density in copper irradiated in this temperature range remains below $1 \times 10^{21}/\text{m}^3$ at least up to damage levels of ~ 1 dpa [33]. According to conventional chemical rate theory predictions, the homogeneous interstitial loop nucleation and growth rates should be similar in Cu and Ni because the interstitial atomic volumes are similar. This suggests that there may be some difference in the initial disposition of interstitials (clustered vs. isolated fraction) produced in displacement cascades in copper compared to nickel. A similar conclusion was reached by Watanabe et al. [45] during their evaluation of in-cascade defect cluster formation in 14-MeV neutron irradiated copper and nickel.

As mentioned in the introduction, molecular dynamics simulations indicate that significant differences exist between the cascade quench behavior of Cu and Ni [3-5]. The MD studies suggest that the duration and affected volume of the "thermal spike" is larger in copper compared to nickel, which results in increased clustering and a lower surviving defect fraction in Cu for a given PKA energy. According to the

observed in these studies may have been formed by diffusion of interstitials following the cascade quench. Figure 12 compares the dose-dependent defect cluster density in copper and nickel irradiated at homologous temperatures between 0.2 and 0.3 T_M [15,44]. The rate of defect cluster accumulation is proportional to the damage level in both copper and nickel at low doses. However, the observed defect cluster density in nickel at a given dose is an order of magnitude smaller in nickel compared to copper. Both materials approach a saturation level in defect cluster density at doses >0.1 dpa. The saturation defect cluster density is apparently a factor of five lower in nickel at low doses. However, However, the observed defect cluster density in nickel at a given dose is an order of magnitude smaller in nickel compared to copper. Both materials approach a saturation level in defect cluster density at doses >0.1 dpa.

thermal spike model, the longer thermal spike lifetime in Cu is due to the lower T_M and less efficient electron-phonon coupling in Cu [3-5,46-49]. Another parameter of interest is the size distribution of defect clusters produced in displacement cascades in copper versus nickel. The size and duration of the thermal spike in copper should result in a larger average cluster size for both vacancies and interstitials. Recent MD studies suggest that small defect clusters containing up to 6 interstitials are highly glissile along $\langle 110 \rangle$ directions [1,50]. Therefore, it seems conceivable that the relative proportioning of interstitial clusters produced in displacement cascades between small, glissile and large, sessile clusters could have a strong influence on the microstructural evolution in metals.

One possible mechanism for the formation of aligned $\{001\}$ defect cluster patterns in irradiated Cu and Ni is based on the propagation of glissile interstitial clusters along $\langle 110 \rangle$ directions. A similar mechanism (based on dynamic crowdion migration) was proposed by Seeger and coworkers [40] to explain the presence of SFT ordered arrays in electron-irradiated FCC metals. However, it seems unlikely that dynamic crowdions could account for the wall formation observed for example in Ni at temperatures between 0.2 and 0.4 T_M since crowdions would not be thermally stable in this temperature regime. From geometric considerations, preferential one-dimensional migration of small interstitial clusters along $\langle 110 \rangle$ directions would lead to the formation of $\{001\}$ walls of vacancy clusters [40]. This potential mechanism for defect cluster patterning suggests that the resistance of copper to form defect cluster walls under energetic displacement cascade conditions could be due to the formation of oversized (sessile) interstitial clusters during the thermal spike. On the other hand, the relatively less efficient interstitial clustering process in nickel during the thermal spike could preferentially produce a larger fraction of small (glissile) interstitial clusters in the displacement cascade. The decreased efficiency of defect clustering in copper irradiated at lower average PKA energies (e.g., 3-MeV protons) could result in a higher fraction of small glissile interstitial clusters, thereby promoting wall formation. Finally, homogeneous nucleation of small interstitial clusters under the high damage rate conditions associated with electron irradiation could also produce a sufficient density of glissile interstitial clusters to induce wall formation.

The low temperature limit in Cu for defect cluster pattern formation during electron irradiation of 0.12 T_M [40] is consistent with the onset of recovery Stage II [51]. Recovery Stage II has generally been attributed to rearrangement of interstitial clusters that either nucleated homogeneously or else directly in the displacement cascade [51]. Diffuse X-ray scattering measurements performed on irradiated FCC metals [51,52] indicate that small interstitial clusters become mobile and coarsen during recovery Stage II.

An alternative explanation for the lack of defect cluster patterning in copper under energetic displacement cascade conditions is associated with the high density of defect clusters produced directly in the displacement cascade. The relatively low fraction of mobile defects (point defects and small defect clusters) and the high sink strength of sessile clusters produced directly in energetic displacement cascades in copper could effectively inhibit the formation of defect cluster patterns. On the other hand, the relatively high fraction of mobile defects and low fraction of sessile defect clusters produced in energetic displacement cascades in nickel could produce conditions favorable for defect cluster patterning. The present study has demonstrated that patterning does not occur in neutron irradiated copper at 50°C at low doses of ~ 0.01 dpa (where defect cluster density is only $\sim 1 \times 10^{21}/\text{m}^3$). This suggests that the relative partitioning between mobile and sessile clusters may be a key parameter for wall formation. The in-cascade production of interstitial defect clusters in Cu should shift from predominantly sessile to predominantly glissile clusters with decreasing PKA energy, which may allow the patterns to form during proton irradiation. One useful test of this hypothesis would be to perform a sequential irradiation of copper involving energetic displacement cascade damage (e.g. neutron irradiation) to introduce a high defect cluster sink density, followed by low-PKA irradiation (e.g., 3-MeV protons).

5. Summary and Conclusions

Despite their similarities in mass, copper and nickel exhibit significantly different responses to energetic particle irradiation. In agreement with previous molecular dynamics and ion irradiation studies, the present study indicates that the magnitude of in-cascade point defect clustering at a given homologous irradiation temperature is lower in neutron irradiated nickel compared to copper. The apparent maximum

visible defect cluster densities in neutron irradiated copper and nickel are $1 \times 10^{24}/\text{m}^3$ and $2 \times 10^{23}/\text{m}^3$, respectively. The high cluster density in copper is due to a high density of SFTs and unidentified small defect clusters (presumably interstitial dislocation loops) produced directly in the displacement cascade. The nucleation and growth of visible interstitial dislocation loops is also much more pronounced in nickel compared to copper. The density of easily resolvable (>5 nm diameter) dislocation loops is two orders of magnitude lower in copper compared to nickel ($1 \times 10^{23}/\text{m}^3$ vs. $1 \times 10^{21}/\text{m}^3$) at damage levels above 0.1 dpa. These dramatic differences in the nature and total density of defect clusters in copper compared to nickel can be rationalized on the basis of a more rapid quenching of the thermal spike phase for energetic displacement cascades in nickel.

The formation of {001} planar arrays of defect clusters at damage levels above 0.1 dpa is a typical feature in Ni irradiated with a wide variety of particles at homologous temperatures between 0.2 and 0.4 T_M , but only occurs in copper for irradiation spectra that produce low-energy PKAs. The sensitivity of Cu to irradiation spectrum is attributed to changes in the fraction of glissile interstitial clusters created at different PKA energies, although the overall lower defect cluster density in Ni may also be playing a role.

The present study provides additional support that significant void swelling ($>0.5\%/dpa$) can occur in copper without the presence of a well-developed dislocation network, in agreement with the production bias void swelling model. Literature data suggest that the steady-state swelling rate in neutron-irradiated Ni is very low ($\sim 0.1\%/dpa$) compared to Cu, despite the presence of a higher network dislocation density that is theoretically more favorable for dislocation bias-driven void swelling.

Acknowledgements

The pure annealed nickel specimens used in this study were supplied by K. Farrell. The irradiated specimens were thinned by L.T. Gibson, W.S. Eatherly and J. Lindbo. This work was supported in part by Risø National Laboratory and by the Office of Fusion Energy, US Department of Energy, under contract DE-AC05-84OR21400 with Martin Marietta Energy Systems, Inc. and contract DE-AC06-76RLO1830 with Battelle Memorial Institute.

References

- [1] S.J. Zinkle and B.N. Singh, *J. Nucl. Mater.* 199 (1993) 173.
- [2] W.J. Phythian, R.E. Stoller, A.J.E. Foreman, A.F. Calder and D.J. Bacon, submitted to *J. Nucl. Mater.*
- [3] T. Diaz de la Rubia, R.S. Averback, H. Hsieh and R. Benedek, *J. Mater. Res.* 4 (1989) 579.
- [4] T. Diaz de la Rubia, R.S. Averback, R. Benedek and I.M. Robertson, *Rad. Eff. Def. Solids* 113 (1990) 39.
- [5] M.W. Finnis, P. Agnew and A.J.E. Foreman, *Phys. Rev. B* 44 (1991) 567.
- [6] G.L. Kulcinski and J.L. Brimhall, in *Effects of Radiation on Substructure and Mechanical Properties in Metals and Alloys*, ASTM STP 529, J. Moteff, ed. (Amer. Soc. for Testing and Materials, Philadelphia, 1973) p. 258
- [7] J.L. Brimhall, Battelle Pacific Northwest Laboratory report BNWL-1839 (1974).
- [8] J.O. Stiegler and K. Farrell, *Scripta Met.* 8 (1974) 651.
- [9] A. Silvent and C. Regnard, 16eme Colloque de Metallurgie INSTN Paris, CEA-CONF-2437 (1974) p. 209.
- [10] J.E. Westmoreland, J.A. Sprague, F.A. Smidt and P.R. Malmberg, *Rad. Eff.* 26 (1975) 1
- [11] P. Regnier and L.D. Glowinski, *J. Nucl. Mater.* 57 (1975) 243.
- [12] J.B. Whitley, Ph.D. Thesis, University of Wisconsin-Madison (1978)
- [13] W. Jäger, P. Ehrhart, W. Schilling, F. Dworschak, A.A. Gadalla and N. Tsukuda, *Mater. Sci. Forum* 15-18 (1987) 881.
- [14] W. Jäger, P. Ehrhart and W. Schilling, *Sol. State Phenom.* 3&4 (1988) 279.
- [15] S.J. Zinkle and L.L. Snead, in *Proc. 17th Int. Conf. on Effects of Radiation on Materials*, *J. Nucl. Mater.*, in press.
- [16] W. Jäger and H. Trinkaus, *J. Nucl. Mater.* 205 (1993) 394.
- [17] C. Abromeit, *Intern. J. Mod. Phys. B* 3 (1989) 1301.

- [18] A.Y. Stathopoulos, *Philos. Mag. A* 44 (1981) 285.; also A.Y. Stathopoulos, C.A. English, B.L. Eyre and P.B. Hirsch, *ibid.* 309.
- [19] M.A. Kirk, I.M. Robertson, M.L. Jenkins, C.A. English, T.J. Black and J.S. Vetrano, *J. Nucl. Mater.* 149 (1987) 21.
- [20] J.S. Vetrano, I.M. Robertson and M.A. Kirk, *Scripta Met.* 24 (1990) 157.
- [21] C.A. English, *Rad. Eff. Def. Solids* 113 (1990) 15.
- [22] I.M. Robertson, J.S. Vetrano, M.A. Kirk and M.L. Jenkins, *Philos. Mag. A* 63 (1991) 299.
- [23] M.L. Jenkins, M.A. Kirk and W.J. Phythian, *J. Nucl. Mater.* 205 (1993) 16.
- [24] I.M. Robertson, D.K. Tappin and M.A. Kirk, *Philos. Mag. A* 68 (1993) 843.
- [25] S-J Kim, M-A Nicolet, R.S. Averback and D. Peak, *Phys. Rev. B* 37 (1988) 38.
- [26] P. Jung, *Phys. Rev. B* 23 (1981) 664.
- [27] C.E. Klabunde and R.R. Coltman, Jr., *J. Nucl. Mater.* 108&109 (1982) 183.
- [28] M.W. Guinan, J.H. Kinney and R.A. Van Konynenburg, *J. Nucl. Mater.* 133&134 (1985) 357.
- [29] G. Wallner, M.S. Anand, L.R. Greenwood, M.A. Kirk, W. Mansel and W. Waschowski, *J. Nucl. Mater.* 152 (1988) 146.
- [30] M. Caro, A. Ardelea and A. Caro, *J. Mater. Res.* 5 (1990) 2652.
- [31] M. Alurralde, A. Caro and M. Victoria, *J. Nucl. Mater.* 183 (1991) 33.
- [32] L.R. Greenwood, *Damage Analysis and Fundamental Studies quarterly progress report DOE/ER-0046/24 (Feb. 1986) p. 5* (the Cu dpa calculations in this report assumed a nonstandard threshold displacement energy of 40 eV).
- [33] S.J. Zinkle, A. Horsewell, B.N. Singh and W.F. Sommer, *J. Nucl. Mater.*, 212-215 (1994) 132.
- [34] S.J. Zinkle, G.L. Kulcinski and R.W. Knoll, *J. Nucl. Mater.* 138 (1986) 46.
- [35] S.J. Zinkle and K. Farrell, *J. Nucl. Mater.* 168 (1989) 262.
- [36] N. Yoshida and M. Kiritani, *J. Phys. Soc. Jap.* 38 (1975) 1220.
- [37] W. Jäger and K. Urban, in *Proc. 4th Int. Conf. on High Voltage Electron Microscopy*, B. Jouffrey and P. Favard, eds. (SFME, Paris, 1976) p. 175.
- [38] H. Fujita, T. Sakata and H. Fukuyo, *Jap. J. Appl. Phys.* 21 (1982) L235.
- [39] N.Y. Yin, F. Phillipp and A. Seeger, *Phys. Stat. Sol. (a)* 116 (1989) 91.
- [40] A. Seeger, N.Y. Jin, F. Phillipp and M. Zaiser, *Ultramicroscopy* 39 (1991) 342.
- [41] ASTM Standard Practice for Neutron Radiation Damage Simulation by Charged-Particle Irradiation, E521-89, *Annual Book of ASTM Standards, Vol. 12.02* (ASTM, Philadelphia).
- [42] H.L. Heinisch and B.N. Singh, *Philos. Mag. A* 67 (1993) 407.
- [43] H. Fukushima, Y. Shimomura and H. Yoshida, *J. Nucl. Mater.* 179-181 (1991) 939.
- [44] B.N. Singh and S.J. Zinkle, *J. Nucl. Mater.* 206 (1993) 212.
- [45] N. Watanabe, R. Nishiguchi and Y. Shimomura, *J. Nucl. Mater.* 179-181 (1991) 905.
- [46] C.P. Flynn and R.S. Averback, *Phys. Rev. B* 38 (1988) 7118.
- [47] A. Caro and M. Victoria, *Phys. Rev. A* 40 (1989) 2287.
- [48] S. Prönnecke, A. Caro, M. Victoria, T. Diaz de la Rubia and M.W. Guinan, *J. Mater. Res.* 6 (1991) 483.
- [49] I. Koponen, *Phys. Rev. B* 47 (1993) 14011.
- [50] A.J.E. Foreman, C.A. English and W.J. Phythian, *Philos. Mag. A* 66 (1992) 655.
- [51] W. Schilling and K. Sonnenberg, *J. Phys. F: Metal Phys.* 3 (1973) 322.
- [52] R. Rauch, J. Peisl, A. Schmalzbauer and G. Wallner, *J. Phys. Condens. Matter* 2 (1990) 9009.
- [53] S.J. Zinkle, *J. Nucl. Mater.* 150 (1987) 140.
- [54] A. Horsewell, B.N. Singh, S. Prönnecke, W.F. Sommer and H.L. Heinisch, *J. Nucl. Mater.* 179-181 (1991) 924.
- [55] T. Muroga, H.L. Heinisch, W.F. Sommer and P.D. Ferguson, *J. Nucl. Mater.* 191-194 (1992) 1150.
- [56] Y. Satoh, I. Ishida, T. Yoshiie and M. Kiritani, *J. Nucl. Mater.* 179-181 (1988) 443.
- [57] S. Kojima, T. Yoshiie and M. Kiritani, *J. Nucl. Mater.* 179-181 (1988) 1249.
- [58] S. Kojima, T. Yoshiie, K. Hamada, K. Satori and M. Kiritani, *J. Nucl. Mater.* 191-194 (1992) 1155.
- [59] N. Yoshida, Y. Akashi, K. Kitajima and M. Kiritani, *J. Nucl. Mater.* 133-134 (1985) 405.
- [60] C.A. English, B.L. Eyre and J.W. Muncie, *Philos. Mag. A* 56 (1987) 453.
- [61] S.J. Zinkle and B.N. Singh, manuscript in preparation
- [62] S. Ishino, *J. Nucl. Mater.* 206 (1993) 139.
- [63] S.J. Zinkle, K. Farrell and H. Kanazawa, *J. Nucl. Mater.* 179-181 (1991) 994.
- [64] M. Kiritani, *Mater. Sci. Forum*, 15-18 (1987) 1023.

- [65] N. Yoshida, T. Muroga, H. Watanabe, K. Araki and U. Miyamoto, *J. Nucl. Mater.* 155-157 (1988) 1222.
- [66] M. Kiritani, T. Yoshiie, S. Kojima, Y. Satoh and K. Hamada, *J. Nucl. Mater.* 174 (1990) 327.
- [67] F.A. Garner and W.G. Wolfer, *J. Nucl. Mater.* 122&123 (1984) 201.
- [68] H.R. Brager, *J. Nucl. Mater.* 141-143 (1986) 79.
- [69] F.A. Garner, M.L. Hamilton, T. Shikama, D.J. Edwards and J.W. Newkirk, *J. Nucl. Mater.* 191-194 (1992) 386.
- [70] J.F. Stubbins and F.A. Garner, *J. Nucl. Mater.* 191-194 (1992) 1295; also J.F. Stubbins, in 17th ASTM Symposium on Effects of Radiation on Materials, D.S. Gelles et al., eds., in press
- [71] B.N. Singh, C.H. Woo and A.J.E. Foreman, *Mater. Sci. Forum* 97-99 (1992) 75.
- [72] H. Trinkaus, B.N. Singh and A.J.E. Foreman, *J. Nucl. Mater.* 206 (1993) 200.